LWT - Food Science and Technology 138 (2021) 110773

Contents lists available at ScienceDirect

LWT

journal homepage: www.elsevier.com/locate/lwt

A new application with characterized oil-in-water-in-oil double emulsions: Gelatin-xanthan gum complexes for the edible oil industry

Turgay Cetinkaya [a,1,*], Filiz Altay [b], Zafer Ceylan [c]

[a] Department of Food Engineering, Graduate School of Science Engineering and Technology, Istanbul Technical University, Istanbul, Turkey
[b] Department of Food Engineering, Faculty of Chemical and Metallurgical Engineering, Istanbul Technical University, Istanbul, Turkey
[c] Department of Gastronomy and Culinary Arts, Faculty of Tourism, Van Yüzüncü Yıl University, Van, Turkey

ARTICLE INFO

Keywords:
Double emulsion
Microencapsulation
Nanoencapsulation
Emulsion stability
Reduced-fat products

ABSTRACT

A novel oil-in-water-in-oil ($O_1/W/O_2$) double emulsion (DE) system was successfully created to decrease the saturated fat content. DEs stabilized with gelatin (GL), xanthan gum (XG), and solid fat crystals were generated using a two-stage emulsification process. Primary emulsions (PEs) containing 60 g/100 g and 20 g/100 g sunflower oil (SFO) were prepared with constant GL (at 1 g/100 g) and XG (at 0.6 g/100 g and 1.4 g/100 g) of the total emulsion, respectively. DEs at constant water concentrations containing SFO at 30, 38.3, 46.7, and 55 g/100 g and different water concentrations at 30, 40, 45, and 60 g/100 g were examined. The DE microstructure showed that SFO was encapsulated in internal water droplets, which were stabilized by interfacial accumulation of fat crystals. The hardness value of the DEs decreased from 13.40 to 3.42 N with increasing SFO. Amplitude and frequency sweep tests revealed a weak gel structure and elastic behavior of DEs. In addition, a decrease in gel stiffness was observed with an increase in SFO and water content. The results of the present study effectively demonstrated a new approach applicable for the edible oil industry, formulating $O_1/W/O_2$ DEs using a natural emulsifier (GL) and a stabilizer (XG).

1. Introduction

Palm oil is used as a hard stock for formulating emulsions and is rich in saturated fats (~49.8 g/100 g) which have negative health effects in terms of their cholesterol profiles (Marangoni & Garti, 2011). Therefore, a number of research have been conducted for structuring liquid oils to reduce saturated fats or *trans*-fats in emulsions (Patel, 2015, 2017; Patel & Dewettinck, 2016). As a new approach, the use of $O_1/W/O_2$ DEs has been considered a promising option. DEs, also known as multiple emulsions, are emulsions in which the dispersed phase itself is an emulsion in the form of fine droplets. In an $O_1/W/O_2$ type emulsion, O_1 and O_2 constitute an internal and external oil phase, respectively. Two distinct interface layers are included: an oil-in-water (O_1–W) layer covering the internal oil droplets and a water-in-oil (W–O_2) layer covering the water droplets (Lamba, Sathish, & Sabikhi, 2015). These systems can be created by one-step (Pradhan & Rousseau, 2012; Yu, Zhu, Hui, & Wang, 2020) and two-step homogenization (Benichou, Aserin, & Garti, 2007; Ji, Deng, Liu, & Qin, 2020; Stasse et al., 2020; Yoshida, Sekine, Matsuzaki, Yanaki, & Yamaguchi, 1999; Zhu, Zheng, Wang, & Wang, 2016) or polymerization (Stasse, Ribaut, Schmitt, & Héroguez, 2019).

Despite its considerable potential, preparation of a stable DE with controlled droplet size is still a significant challenge compared to standard emulsions (McClements, 2010). In particular, $O_1/W/O_2$ DE systems are susceptible to different types of instabilities such as flocculation, creaming, and Ostwald ripening (Benichou et al., 2007; Chávez-Páez, Quezada, Ibarra-Bracamontes, González-Ochoa, & Arauz-Lara, 2012; McClements, 2010; Muschiolik, 2007). One way to obtain stable DEs is to use synthetic emulsifiers (Dickinson, 2011; Mun et al., 2010). However, high concentrations of petroleum-based surfactants are strongly restricted by food organizations. Hence, the structuring DEs via gelation of the aqueous phase or solidification of the oil phase have used recently for reduction or eliminating surfactants. Researchers have also focused on formulating DEs stabilized by biopolymer complexes. In this study, protein-polysaccharide complexes gained more attention to stabilize DEs (Bouyer, Mekhloufi, Rosilio, Grossiord, & Agnely, 2012; Jahaniaval, Kakuda, & Abraham, 2003; Patel, 2017). For instance, $O_1/W/O_2$ DEs using soluble and insoluble whey protein concentrate-gum arabic

* Corresponding author.
E-mail address: turgay.cetinkaya@yalova.edu.tr (T. Cetinkaya).
[1] Present Address: Food Processing Department, Armutlu Vocational School, Yalova University, 77500, Yalova, Turkey.

https://doi.org/10.1016/j.lwt.2020.110773
Received 22 July 2020; Received in revised form 10 December 2020; Accepted 13 December 2020
Available online 15 December 2020
0023-6438/© 2020 Elsevier Ltd. This is an open access article under the CC BY-NC-ND license (http://creativecommons.org/licenses/by-nc-nd/4.0/).

Table 1
The compositions of PEs.

Sample no.	O_1/W ratio	Oil phase (O_1)	Water phase	
		SFO (g/100 g)	GL solution (g/100 g)	XG solution (g/100 g)
I[a]	60/40	60	10	30
II[b]	20/80	20	10	70

[a] Contains 1 g/100 g GL and 0.6 g/100 g XG.
[b] Contains 1 g/100 g GL and 1.4 g/100 g XG.

Table 2
The compositions of DEs.

Sample no.	$O_1/W/O_2$ (g/100 g)	O_1/W emulsion (g/100 g)	Added oils (g/100 g)	
	$O_1/W/O_2$	**60/40 (Sample I)**	**Palm oil (O_2)**	**SFO (O_1)**
III	30/20/50	50	50	–
IV	38.3/20/41.7	50	41.7	8.3
V	46.7/20/33.3	50	33.3	16.7
VI	55/20/25	50	25	25
	$O_1/W/O_2$	**20/80 (Sample II)**	**Palm oil (O_2)**	
VII	7.5/30/62.5	37.5	62.5	-
VIII	10/40/50	50	50	-
IX	11.25/45/43.75	56.25	43.75	-
X[a]	15/60/25	75	24.6	-

[a] Contains 0.4 g/100 g PGPR.

complexes (Estrada-Fernández et al., 2018) or sodium caseinate, carrageenan, and soy lecithin (Thanh Diep et al., 2018) were successfully produced.

The co-existence of hydrophilic and hydrophobic parts in the structure of proteins, such as in GL, makes them natural emulsifiers with high functionality for stabilizing W/O or O/W interfaces in food emulsions. Furthermore, a combination of some polysaccharides (such as XG with GL) were applied to modify complex emulsion microstructures, strengthening the protein network formed at the oil interface (Benichou et al., 2007; Patel, 2015; Wilde, Mackie, Husband, Gunning, & Morris, 2004), through hydrophobic reactions and non-coulombic interactions involving NH and OH groups (Lii, Liaw, Lai, & Tomasik, 2002). Therefore, XG–GL matrices are appropriate and promising candidates to design stable multiple structured emulsions.

In this study, $O_1/W/O_2$ DEs were prepared by fat crystallization using a two-stage emulsification method to obtain reduced-fat emulsions. In the first step PE, O_1/W was formulated using SFO, were stabilized with XG and GL complexes. In the second step, palm oil was added to the PE to obtain a structured $O_1/W/O_2$ DE system. These complex systems have considerable potential in food applications for encapsulating oils as hydrophobic compounds, and for designing and texturing reduced-fat food products.

2. Materials and methods

2.1. Materials

Type B GL with a molecular weight of about 50 000 g/mol (sample No 315–0807), was received from PB Gelatins GmbH, a member of the Tessenderlo Group (Brussel, Belgium). XG (SATIAXANE CX 801 LOT R253544) was obtained from Cargill (Redon, France). SFO was purchased from Vandemoortele R&D (Izegem, Belgium). Palm oil was provided by Vandermoortele N.V. (Izegem, Belgium) and melted at 50 °C before use. GRINDSTED® polyglycerol-polyricinoleate (PGPR) was obtained from DuPont Nutrition & Health (Copenhagen, Denmark). Distilled water was used for the experiments.

2.2. Methods

2.2.1. Preparation of PEs and DEs

Weighted amounts of GL and XG powders were dispersed in distilled water at 10 g/100 g and 2 g/100 g, respectively. These concentrations were selected based on previous reports (Patel, 2017; Patel et al., 2015). Complete dissolution was obtained continuously stirring GL solutions at 50 °C and XG solutions at room temperature (25 ± 3 °C). To prepare the PEs (O_1/W), SFO was added to the mixed solution and then homogenized with Ultraturrax (T 25 B, IKA-Werke GmbH & Co. KG, Breisgau, Germany) at 11 000 rotations per minute (rpm) for 3 min. A summary of the two-step emulsification procedure is provided in Supplementary material 1. (S1). The prepared O_1/W PEs with ratios of 60:40 and 20:80 were applied as templates to fabricate $O_1/W/O_2$ DEs (Table 1). The DE compositions are listed in Table 2 and prepared using the following two methods.

Method 1: The 60:40 PE was blended with melted palm oil/SFO and homogenized using Ultraturrax first at 11 000 rpm for 2 min and then at 13 000 rpm for 6 min to obtain samples III, IV, V, and VI.

Method 2: The 20:80 PE was homogenized with melted palm oil at different ratios using Ultraturrax at 8000 rpm for 6 min and then at 4000 rpm for 4 min to obtain samples VII, VIII, IX, and X. PGPR was added to sample X at 0.4 g/100 g. During homogenization, the temperature of all samples was decreased by using an ice bath to crystallize the palm oil. All samples were kept at 4 °C until further analysis.

2.2.2. Optical microscope

To visualize the microstructure of the emulsions, optical microscopic imaging under normal and polarized light was conducted using a microscope (Leica DM 2500, Leica Microsystems, Wetzlar, Germany) equipped with a color camera (Leica MC 170HD). A drop of the freshly prepared sample was placed on a microscope slide and covered with a cover slip. The imaging was performed at 25 °C. The average diameters were determined by measuring 50 random water globules using Image J program (National Institutes of Mental Health, Bethesda, Maryland, USA).

2.2.3. Cryogenic scanning electron microscopy

The morphology of the emulsions and network of polymers in the bulk phase and at the droplet interface were observed by cryogenic scanning electron microscopy (Cryo-SEM). The samples were placed in the slots of a stub, plunge-frozen in liquid nitrogen and transferred into the cryo-preparation chamber (PP3010T Cryogenic-SEM preparation systems, Quorum Technologies, Lewes, UK) where they were freeze-fractured. After fracture, the samples were sputter-coated with Pt and examined with a SEM (JSM 7100 F, JEOL Ltd, Tokyo, Japan). The minimum, maximum and average diameters were determined by open source processing program Image J.

2.2.4. Droplet size distribution

The droplet size distribution (DSD) of PEs was determined using a dynamic light scattering instrument (Mastersizer 3000, Malvern, Worcestershire, UK) at 20 °C. The samples were diluted with distilled water. The refractive indices of SFO and water were 1.52 and 1.33, respectively. The droplet size distribution was expressed as the mean droplet size and volume-weighted mean diameter [$D_{4,3}$]. All experiments were conducted in triplicate.

2.2.5. Rheological measurements

The rheological behavior of the fabricated DEs was measured using a rheometer (TA Instruments, AR 2000 ex, USA) equipped with a parallel-plate cross-hatched geometry (diameter = 40 mm, gap = 1000 μm) sensor system. Dynamic oscillatory measurements were conducted in the linear viscoelastic region (LVR), where rheological properties are not stress dependent. Amplitude sweep measurements were performed in the range of 0.1–3000 Pa at 1 Hz, in order to determine the LVR for the

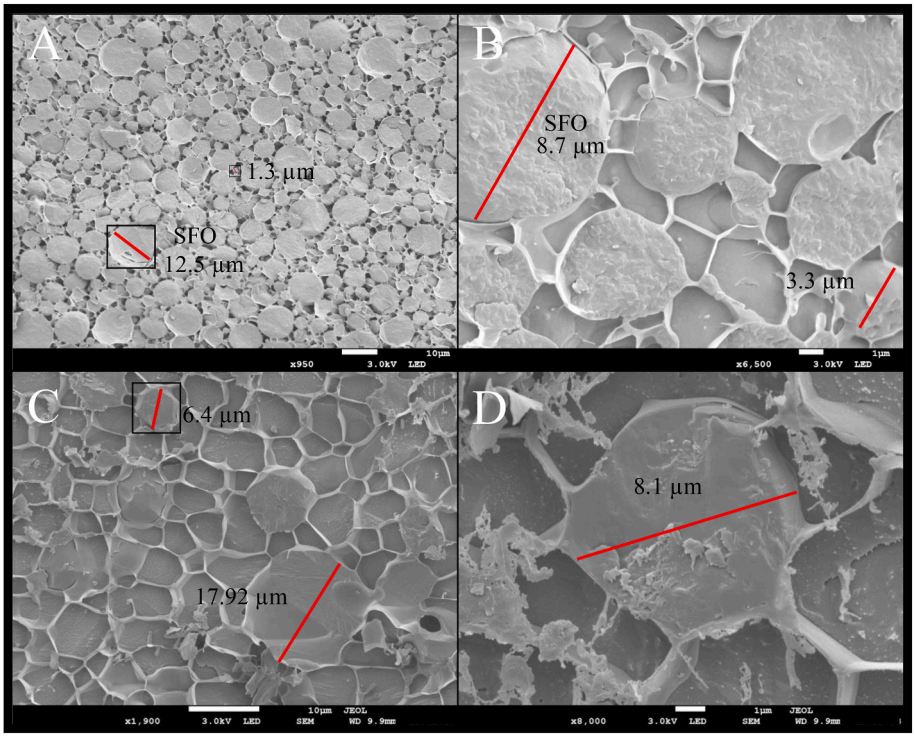


Fig. 1. Cryo-SEM images of PEs.

samples. Frequency sweep was carried out between 0.1 and 100 Hz. The storage (elastic) modulus G′ was obtained as a function of frequency. Rheological measurements were performed in triplicate at 20 °C for samples III, IV, V, VI, and at 10 °C for samples VII, VIII, IX, and X.

2.2.6. Hardness measurements

The hardness of the DEs was determined using a texture profile analyzer (Lloyd Instruments, A 5942 Instron TA 500, Bognor Regis, West Sussex, UK). The samples were kept at 4 °C for overnight. A cylindrical probe (diameter = 11 mm) was inserted into the sample to a depth of approximately 20 mm at a rate of 1 mm/s with a 0.1 N (N) trigger value. Measurements were conducted four times for each sample.

2.2.7. Differential scanning calorimetry measurements

The thermal behavior of the DEs was measured using a differential scanning calorimetry (DSC) (TA Instruments, Q1000, New Castle, DE) two weeks after their preparation. The temperature ranged from 6 to 95 °C at 5 K/min. The DSC was calibrated with indium (TA Instruments, New Castle, DE), azobenzene (Sigma-Aldrich Bornem, Belgium), and undecane (Acros Organics, Geel, Belgium) before analysis. Samples (5–10 mg) were placed into aluminum pans and hermetically sealed. An empty pan was used as the reference. The measurements were performed in triplicate. The peak starting temperature (T_o), peak temperature (T_p), peak end temperature (T_e), heat energy (ΔH) values Supplementary material 3. (S3) were determined from the thermograms using TA Universal Analysis Software (TA Instruments, New Castle, DE).

2.2.8. Statistical analysis

Hardness and DSD values, rheological and thermal properties were analyzed by IBM SPSS Statistics Program (21st version) using one-way analysis of variance (ANOVA) at 0.05 level of significance. Tukey's new multiple range test was applied as a post hoc test. The differences between all samples were evaluated statistically ($p < 0.05$). The results are reported as the mean value ± SD.

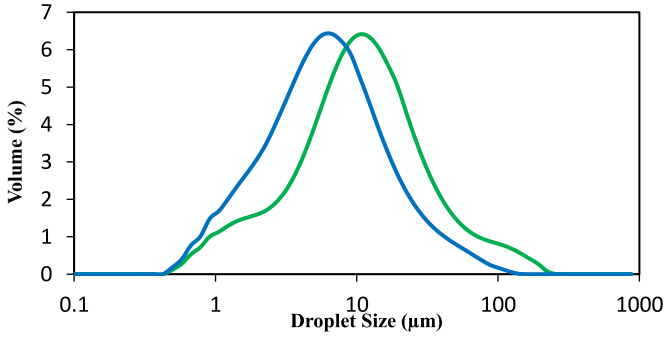


Fig. 2. Droplet size distribution curves of O_1/W PEs. 0.6 g/100 g XG (Sample I); 1.4 g/100 g XG (Sample II).

3. Results and discussion

3.1. Microstructure of PEs

The images of the PEs (Fig. 1 and S2.) showed that there were fewer SFO droplets when the oil phase was decreased from 60 g/100 g (sample I: Fig. 1A and B) to 20 g/100 g (sample II: Fig. 1C and D). In this respect, the minimum and maximum diameters of A were determined as 1.3 µm and 12.5 µm, respectively. Also, those of B samples were found to be 3.3 µm and 8.7 µm. As can be seen from the results, the results obtained from A and B images were in the same scope. The range of C samples was determined between 17.92 µm and 6.4 µm. The diameter of D sample was found as 8.1 µm. It was revealed that C and D obtained from 1.4 g/100 g XG were in the same range as can be seen from the results of the average diameters. So, it could be concluded that the average diameters might have been increased because of the fact that XG concentration was increased.

Cryo-SEM images confirmed that oil droplets were connected via a network of distinct polymer layers (GL-XG) after the removal of the water phase. The network of polymers in the bulk phase and the

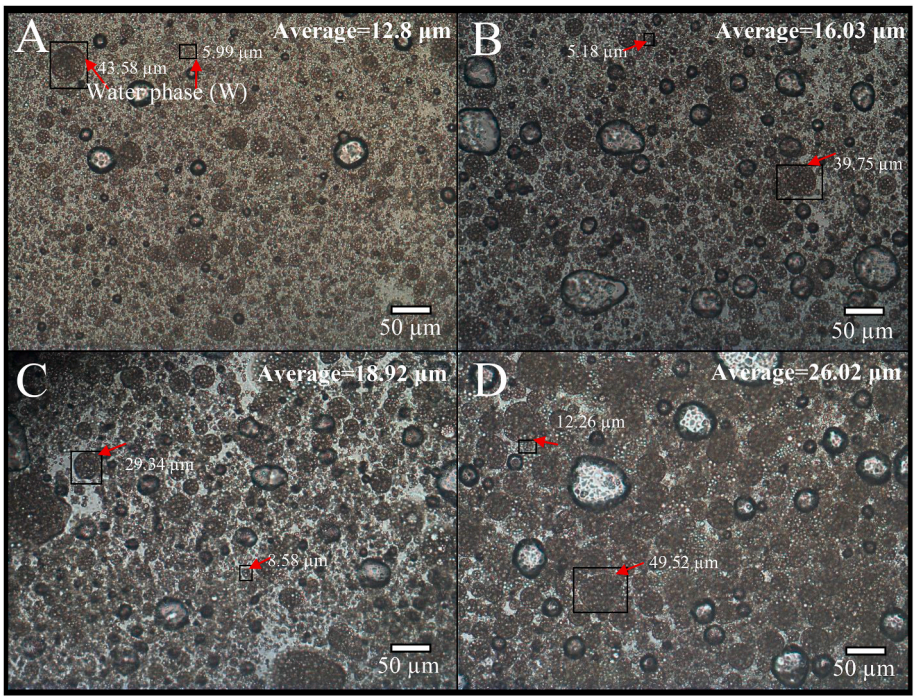


Fig. 3. Optical microscopy images of DEs.

presence of distinct interfaces confirmed that increasing the XG amount from 0.6 to 1.4 g/100 g resulted in a more complex network in the bulk phase and at the interphase. These results agree with a study reporting that highly viscous XG is an effective thickener even at low concentrations (Li Yuet Hee, Jacquot, Hardy, & Desobry, 2008). The stabilization was attributed to the XG-GL layer surrounding the SFO droplets.

3.2. Droplet size distribution of PEs

The DSD of the PEs is displayed in Fig. 2. As could be seen from the area of the figure, the droplet size of XG obtained from 1.4 g/100 g (sample II) was found to be higher than sample I (0.6 g/100 g). Also, the volume weighted mean droplet sizes [$D_{4,3}$] were measured as 9.22 ± 2.29^{a} (sample I) and 17.21 ± 1.05^{b} (sample II), respectively. Patel (2017) noted that XG is required for improving the viscoelastic properties of PE, using it as a stabilizing agent to avoid phase separation. The

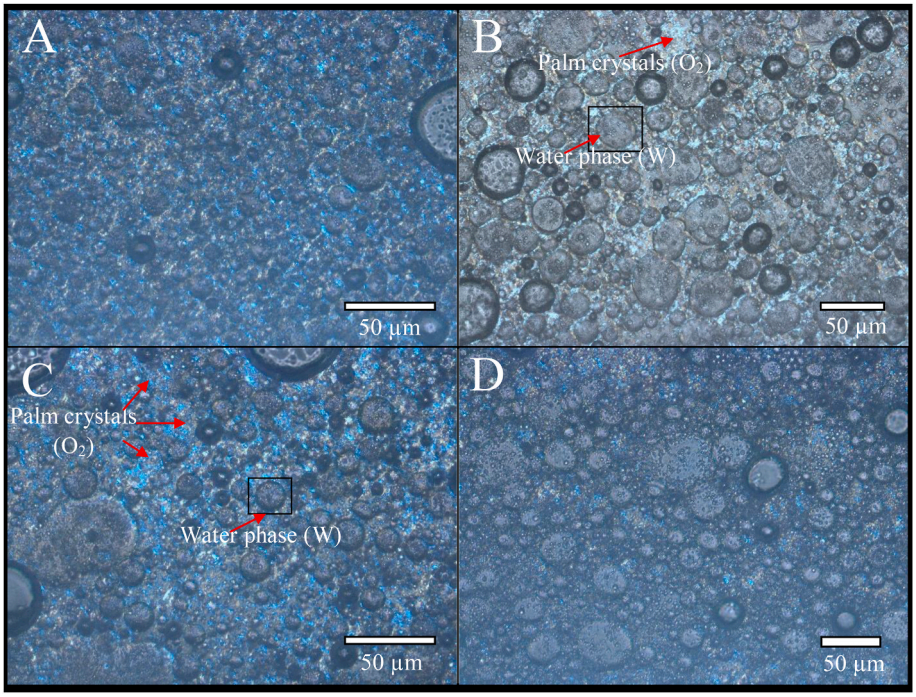


Fig. 4. Palm crystalline network formation of $O_1/W/O_2$ DEs under polarized light microscope. Blue colors represent solidified palm oils (O_2) after cold homogenization process. (For interpretation of the references to color in this figure legend, the reader is referred to the Web version of this article.)

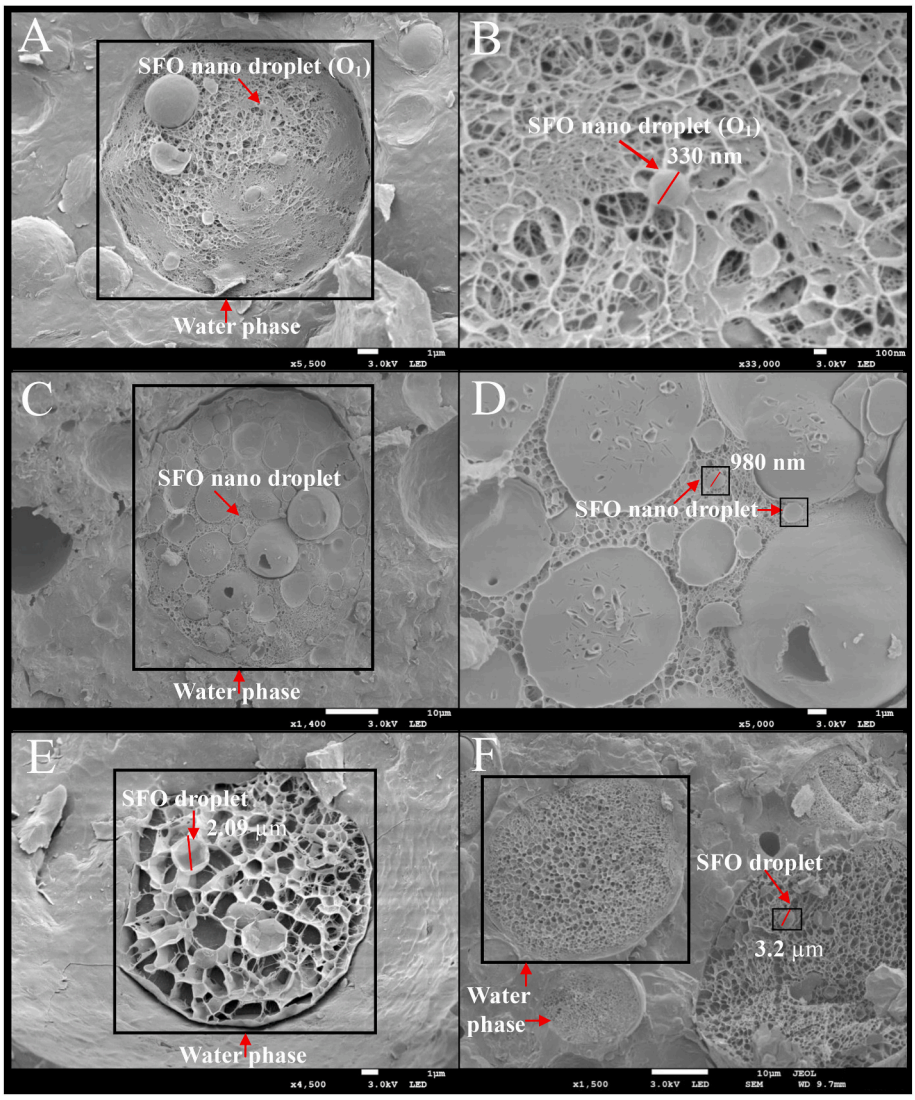


Fig. 5. Cryo-SEM images of DEs.

reason for the higher [$D_{4,3}$] values of sample II are attributed to higher viscosity.

3.3. Optical and polarized light microscope images of DEs

The microstructure of the DEs illustrated the encapsulated liquid SFO in clusters of water droplets (Fig. 3). Average values calculated from fifty different values were obtained for each figure. As could be seen from the obtained results, differences were found between the four different applications in the frame of average values. The average values given with standard deviations of A (sample III), B (sample IV), C (sample V), and D (sample VI) samples in Fig. 3 have been identified as 12.8 ± 6.8 µm, 16.03 ± 6.85 µm, 18.92 ± 6.11 µm, and 26.02 ± 9.91 µm, respectively. The solid fat was replaced with liquid SFO in the presence of natural emulsifiers, which could be important for the edible oil industry. Stable DEs could be prepared replacing as much as 25 g/100 g palm oil with SFO. A lower palm oil concentration resulted in phase separation, suggesting that a minimum of 25 g/100 g palm oil is required to form a stable DE without coalescence. Patel (2017) reported that stabilizing the interfaces by in situ crystallization provides better stability compared to pre-formed crystals. When crystallization was carried out with homogenization, stable PE droplets (O_1/W) were obtained in the external oil phase (O_2) (Patel, 2017). Polarized light microscopy images indicated in Fig. 4A–D (sample VII-X) that a stable emulsion was created by interfacial and bulk crystallization of semisolid fat and the water phase. DEs with <1 µm SFO in water globules were surrounded by a blue fat crystal network (solidified palm oil). When the palm oil was decreased, the blue color of the figures was accordingly decreased, as could be seen in figures. A was found to be more stable because of the fact that water content was lower as compared to the other figures (B and C: but excluding D captured by PGPR). The less spherical shape and higher droplet size corresponded to lower stability in Fig. 4C (45 g/100 g). The addition of PGPR ensured the dispersion of water into fine droplets at 60 g/100 g water, and bulk crystallization occurred at the interfaces providing a stable DE (Fig. 4D). Thanh Diep et al. (2018) also successfully stabilized O_1/W/O_2 DEs up to 60 g/100 g water content using sodium caseinate, k-carrageenan, and soy lecithin.

DEs stabilized with natural emulsifiers need a certain level of solid fats in the outer phase to form a crystal network surrounding water droplets for long storage (Jahaniaval et al., 2003; Pradhan & Rousseau, 2012). In this study, it was observed that palm oil significantly affected the stability of emulsions. The microstructure did not change after 7 days of storage at a 30 g/100 g water concentration. With 40 g/100 g water, quite a number of internal water droplets remained even after 60 days of storage. Thanh Diep et al. (2018) revealed that the structure of O_1/W/O_2 DEs comprising 2:8 O/W was unchanged after 4 weeks of

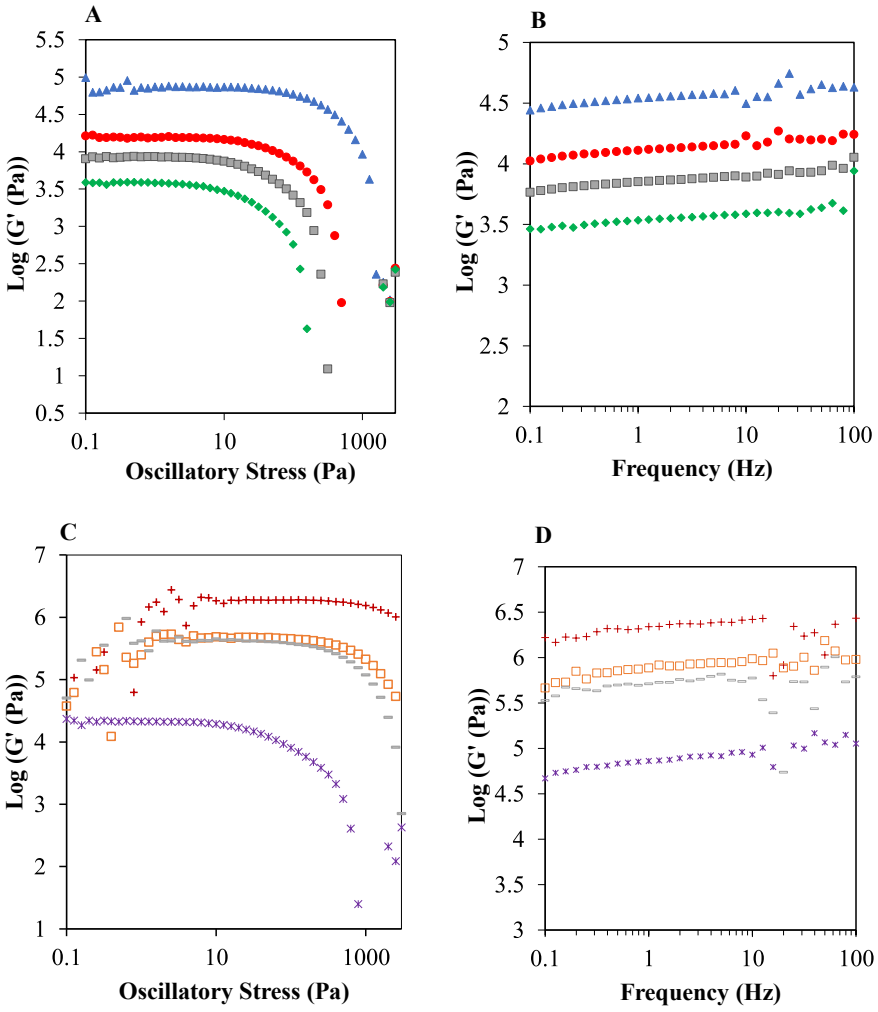


Fig. 6. G′ plotted against oscillatory stress and frequency sweeps. (A, B): ▲ Sample III, ● Sample IV, ■ Sample V, ◆ Sample VI; (C, D): (+ Sample VII, □ Sample VIII, ▬ Sample IX, × Sample X).

storage at 5 °C. On the 14th day of the storage, slight droplet deformation and outer droplet coalescence were observed in some parts by increasing the water content to 45 g/100 g. A small number of droplets aggregated to a nonspherical shape, inducing the coalescence (Pays, Giermanska-Kahn, Pouligny, Bibette, & Leal-Calderon, 2001; Stasse et al., 2020). When the water ratio was increased to 60 g/100 g in storage after 40 days, there was phase separation despite the use of 0.4 g/100 g PGPR, and the amount of DE was decreased.

3.4. Cryogenic scanning electron microscopy images of DEs

As shown in Fig. 5, SFO droplets (marked by red arrows) are interconnected via a network of GL-XG mixtures (Sample VII: A and B; Sample VIII: C and D; Sample IX: E; Sample X: F). The Cryo-SEM images of freeze-fractured DEs confirmed a high inner oil droplet encapsulation due to the process involved in DE formation and the breakdown of the PE macrophase into discrete droplets as reported in another study (Patel, 2017). A closer look at the enlarged image for sample VII (B) shows that the SFO size is approximately 330 nm. The SFO droplet size increased up to 3.2 μm as the water amount went up to 60 g/100 g.

3.5. Rheological behavior

The storage modulus (G′) values were determined in the LVR for each sample at different SFO and water concentrations. The G′ was lower at higher SFO concentration (Fig. 6A). The shorter straight line with increasing SFO concentration indicated a lower stability and reduced DE strength (Thanh Diep et al., 2018). Fig. 6B shows a slight positive slope in the present study, which indicated a weak gel structure of the emulsions. This was probably due to decreasing amount of palm oil. G′ values of samples III-VI showed the effect of SFO substation for palm oil on the stability of DEs at the constant water contents. The highest G′ value was belonged to sample III which containing 50 g/100 g palm oil. The increasing SFO substitution for palm oil decreased the G′ values. However, this decrease was not dramatic as G′ values of sample VI was 3.5 Pa for half of the palm oil was substituted with SFO.

The increasing water phase decreased the gel strength at 10 °C for samples VII-X (Fig. 6C). The weak gel structure of DEs weakened with increasing water content, especially for the sample X which even containing PGPR and a higher ratio of GL and XG compared to other samples (Fig. 6D). However, all G′ values of samples at 10 °C (Fig. 6D) were higher than G′ values presented in Fig. 6B, probably due to low temperature. It is interesting to note that the G′ values of samples VII and X

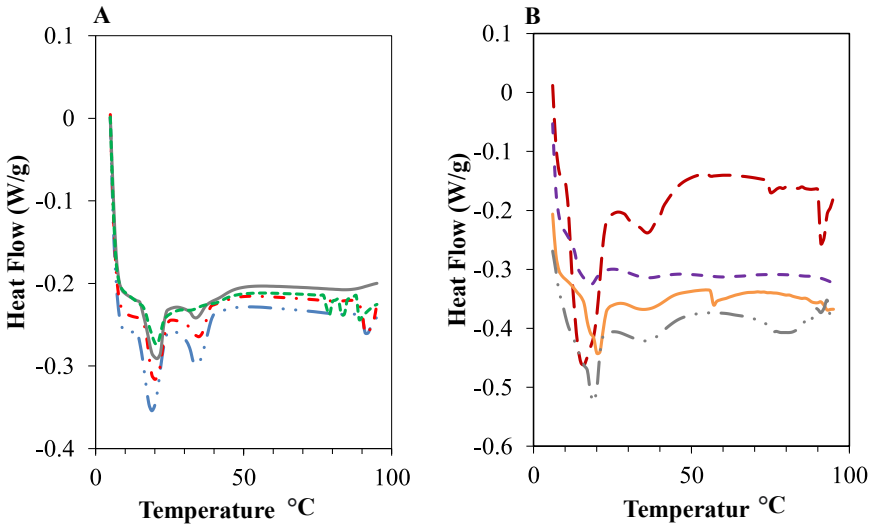


Fig. 7. DSC spectra plotted as heat flow against temperature. (A): Sample III, Sample IV, Sample V, 4 Sample VI; (B): Sample VII, Sample VIII, Sample IX, Sample X.

are different than each other as their water contents have almost 30 g/100 g difference, while samples VIII and IX containing 40 g/100 g and 45 g/100 g water contents, respectively, have high G′ values as samples VII compared to sample X. It appears that samples VIII and IX have both high-water contents and relatively stable structures in terms of their module values. The results were in accordance with the study of Thanh Diep et al. (2018), reported that increasing water and SFO concentrations affected the DE stability.

3.6. Hardness

Replacement of palm oil with SFO decreased the internal strength similar to G′ values of samples. The hardness of the DEs for samples III, IV, V, and VI were 13.40 ± 1.68^{a} N, 9.70 ± 2.13^{bc} N, 8.12 ± 0.70^{bc} N, and 3.42 ± 0.61^{d} N, respectively. The hardness for samples VII, VIII, IX, and X were 58.99 ± 6.45^{A} N, 27.47 ± 4.43^{B} N, 39.04 ± 2.13^{C} N, and 6.32 ± 0.67^{D} N, respectively.

The lower gel stiffness with increasing water concentrations confirm the effect of water incorporation onto the stiffness and internal strength of the emulsion structure as described by Patel (2017). Thus, hardness, can be decreased using SFO and water, which is important for the consumer.

3.7. Thermal behavior

The endothermic thermograms of samples were presented in Fig. 7. The first endothermic melting peak was intense and also associated with eutectic melting point. In contrast to the first endothermic melting peak, the second one is defined as the progressive melting point. The thermograms obtained by heating revealed that DEs melt in the range of 15–20 °C (Dalmazzone, Noïk, & Clausse, 2009). In Fig. 7A, the first peaks decreased as decreasing palm oil content, whereas the second peaks decreased with increasing SFO content. In the second thermogram, the melting exotherm (two peaks) shifted to higher temperatures at 40 g/100 g water concentration (Fig. 7B). It was demonstrated that the melting temperature depended on the type and concentration of the emulsifier (Zafeiri, Smith, Norton, & Spyropoulos, 2017). Zafeiri et al. (2017) reported melting events at higher temperatures for SFO based O/W emulsions when acetyl palmitate (2.5 g/100 g) was used in the presence of sodium caseinate (0.8 g/100 g). According to all results of the present study, the lower melting temperatures have been attributed to the lower emulsifier amount.

4. Conclusion

Optical images revealed that stable oil-in-water emulsions with spherical SFO shapes in the water phase were effectively obtained. In addition, cryo-SEM results showed that SFO droplets were successfully connected via a network of distinct layers of GL-XG. The droplet size of PE was higher when the XG used at 1.4/100 g compared to 0.6 g/100 g. The two-step emulsification method was very efficient encapsulating SFO with the XG-GL mixture. The DEs remained stable at 40 g/100 g water phase content even after 60 days of storage. Replacement of palm oil with SFO, increased the average diameter of water globules. In terms of rheological behavior of the DEs, lower palm oil content weakened the gel structure and increasing the SFO and water content relative to palm oil resulted in an increased deformation. In addition, increasing the SFO successfully decreased the hardness, which could be important for consumer acceptance. The present study plays a guiding role for further studies on DEs at micro or nanoscale, which is relevant to the edible oil industry.

CRediT authorship contribution statement

Turgay Cetinkaya: Data curation, Formal analysis, Investigation, Writing - original draft, preparation. **Filiz Altay:** Supervision, Writing - review & editing. **Zafer Ceylan:** Supervision, Writing - review & editing.

Declaration of competing interest

The authors declare that there are no conflicts of interest.

Acknowledgements

This study was adapted from Turgay Cetinkaya's MSc thesis. All laboratory facilities and chemicals were provided by Ghent University. The authors thank Ashok Patel, who regrettably passed away, for the idea and concept of this work. Mohd Dona Bin Sintang and Lien Vermier are thanked for experimental assistance.

Appendix A. Supplementary data

Supplementary data to this article can be found online at https://doi.org/10.1016/j.lwt.2020.110773.

References

Benichou, A., Aserin, A., & Garti, N. (2007). O/W/O double emulsions stabilized with WPI-polysaccharide conjugates. *Colloids and Surfaces A: Physicochemical and Engineering Aspects, 297*, 211–220.

Bouyer, E., Mekhloufi, G., Rosilio, V., Grossiord, J. L., & Agnely, F. (2012). Proteins, polysaccharides, and their complexes used as stabilizers for emulsions: Alternatives to synthetic surfactants in the pharmaceutical field? *International Journal of Pharmaceutics, 436*, 359–378.

Chávez-Páez, M., Quezada, C. M., Ibarra-Bracamontes, L., González-Ochoa, H. O., & Arauz-Lara, J. L. (2012). Coalescence in double emulsions. *Langmuir, 28*, 5934–5939.

Dalmazzone, C., Noïk, C., & Clausse, D. (2009). Application of DSC for emulsified system characterization. *Oil & Gas Science and Technology - Revue de l'IFP, 64*, 543–555.

Dickinson, E. (2011). Double emulsions stabilized by food biopolymers. *Food Biophysics, 6*, 1–11.

Estrada-Fernández, A. G., Román-Guerrero, A., Jiménez-Alvarado, R., Lobato-Calleros, C., Alvarez-Ramirez, J., & Vernon-Carter, E. J. (2018). Stabilization of oil-in-water-in-oil (O1/W/O2) Pickering double emulsions by soluble and insoluble whey protein concentrate-gum Arabic complexes used as inner and outer interfaces. *Journal of Food Engineering, 221*, 35–44.

Jahaniaval, F., Kakuda, Y., & Abraham, V. (2003). Characterization of a double emulsion system (oil-in-water-in-oil emulsion) with low solid fats: Microstructure. *Journal of the American Oil Chemists' Society, 80*(1), 25–31.

Ji, J., Deng, C., Liu, X., & Qin, J. (2020). Fabrication of porous polyimide hollow microspheres through O/W/O multiple emulsion. *Colloids and Surfaces A: Physicochemical and Engineering Aspects, 591*, 124537.

Lamba, H., Sathish, K., & Sabikhi, L. (2015). Double emulsions: Emerging delivery system for plant bioactives. *Food and Bioprocess Technology, 8*, 709–728.

Li Yuet Hee, L., Jacquot, M., Hardy, J., & Desobry, S. (2008). Formulating polymeric gels simulating soft cheeses' texture. *Food Hydrocolloids, 22*, 925–933.

Lii, C. Y., Liaw, S. C., Lai, V. F., & Tomasik, P. (2002). Xanthan gum-gelatin complexes. *European Polymer Journal, 38*, 1377–1381.

Marangoni, A. G., & Garti, N. (2011). *Edible oleogels: Structure and health implications*. Urbana, IL: AOCS Press.

McClements, D. J. (2010). Emulsion design to improve the delivery of functional lipophilic components. *Annual Review of Food Science and Technology, 1*, 241–269.

Mun, S., Choi, Y., Rho, S.-J., Kang, C.-G., Park, C.-H., & Kim, Y.-R. (2010). Preparation and characterization of water/oil/water emulsions stabilized by polyglycerol polyricinoleate and whey protein isolate. *Journal of Food Science, 75*, E116–E125.

Muschiolik, G. (2007). Multiple emulsions for food use. *Current Opinion in Colloid & Interface Science, 12*, 213–220.

Patel, A. R. (2015). *Alternative routes to oil structuring*. New York: Springer International Publishing.

Patel, A. R. (2017). Surfactant-free oil-in-water-in-oil emulsions stabilized solely by natural components-biopolymers and vegetable fat crystals. *MRS Advances, 2*, 1095–1102.

Patel, A. R., & Dewettinck, K. (2016). Edible oil structuring: An overview and recent updates. *Food and Function, 7*, 20–29.

Patel, A. R., Rajarethinem, P. S., Cludts, N., Lewille, B., De Vos, W. H., Lesaffer, A., et al. (2015). Biopolymer-based structuring of liquid oil into soft solids and oleogels using water-continuous emulsions as templates. *Langmuir, 31*, 2065–2073.

Pays, K., Giermanska-Kahn, J., Pouligny, B., Bibette, J., & Leal-Calderon, F. (2001). Coalescence in surfactant-stabilized double emulsions. *Langmuir, 17*, 7758–7769.

Pradhan, M., & Rousseau, D. (2012). A one-step process for oil-in-water-in-oil double emulsion formation using a single surfactant. *Journal of Colloid and Interface Science, 386*, 398–404.

Stasse, M., Laurichesse, E., Ribaut, T., Anthony, O., Héroguez, V., & Schmitt, V. (2020). Formulation of concentrated oil-in-water-in-oil double emulsions for fragrance encapsulation. *Colloids and Surfaces A: Physicochemical and Engineering Aspects, 592*, 124564.

Stasse, M., Ribaut, T., Schmitt, V., & Héroguez, V. (2019). Encapsulation of lipophilic fragrance by polymerization of the intermediate aqueous phase of an oil-in-water-in-oil (O/W/O) double emulsion. *Polymer Chemistry, 10*, 4154–4162.

Thanh Diep, T., Phan Dao, T., Vu, H. T., Quoc Phan, B., Ngoc Dao, D., Huu Bui, T., et al. (2018). Double emulsion oil-in water-in oil (O/W/O) stabilized by sodium caseinate and k-carrageenan. *Journal of Dispersion Science and Technology, 39*, 1752–1757.

Wilde, P., Mackie, A., Husband, F., Gunning, P., & Morris, V. (2004). Proteins and emulsifiers at liquid interfaces. *Advances in Colloid and Interface Science, 108*, 63–71.

Yoshida, K., Sekine, T., Matsuzaki, F., Yanaki, T., & Yamaguchi, M. (1999). Stability of vitamin A in oil-in-water-in-oil-type multiple emulsions. *Journal of the American Oil Chemists' Society, 76*, 1–6.

Yu, H., Zhu, Y., Hui, A., & Wang, A. (2020). Preparation of porous microspherical adsorbent via pine pollen stabilized O1/W/O2 double emulsion for high-efficient removal of cationic dyes. *Colloids and Surfaces A: Physicochemical and Engineering Aspects, 601*, 124997.

Zafeiri, I., Smith, P., Norton, I. T., & Spyropoulos, F. (2017). Fabrication, characterisation and stability of oil-in-water emulsions stabilised by solid lipid particles: The role of particle characteristics and emulsion microstructure upon Pickering functionality. *Food and Function, 8*, 2583–2591.

Zhu, Y., Zheng, Y., Wang, F., & Wang, A. (2016). Fabrication of magnetic porous microspheres via (O1/W)/O2 double emulsion for fast removal of Cu2+ and Pb2+. *Journal of the Taiwan Institute of Chemical Engineers, 67*, 505–510.